PROCEEDINGS OF THE IV INTERNATIONAL CONFERENCE/HIGH TEMPERATURE CAPILLARITY

JOURNAL OF MATERIALS SCIENCE **40** (2005) 2525–2529

Mathematical model for simultaneous growth of gas and solid phases in gas-eutectic reaction

L. DRENCHEV*
Institute of Metal Science, 67 Shipchenski Prohod Street, 1574 Sofia, Bulgaria
E-mail: ljudmil.d@ims.bas.bg

J. SOBCZAK
Foundry Research Institute, 73 Zakopianska Street, 30-418 Krakow, Poland

W. SHA, S. MALINOV
Queen's University of Belfast, Belfast, BT7 1NN, UK

Simultaneous growth of solid and gas phases from gas supersaturated melt is the basis of a relatively new method for the production of ordered porosity materials. Such phase transformation is called gas-eutectic reaction. The structure obtained mainly depends on thermal and gas diffusion phenomena at solid/liquid interface. It is difficult to control this phase transformation but it is very important to the eventual structure. The development of a general mathematical model of the entire physical process will help for better understanding of the structure formation and will allow effective control to be provided. This paper presents a mathematical description of the complex physical phenomena during gas-eutectic transformation. Analyses for heat transfer, solidification kinetics and gas diffusion were coupled to describe the formation of the gas reinforced structure. The model was applied for simulation of structures after some special processing regimes. The structure sensitivity with respect to the different components of gas pressure is discussed.

1. Introduction

Depending on the metal nature, pores form during solidification due to shrinkage phenomenon and higher gas solubility in molten phase compared with that in solid phase. One of the most effective ways to reduce pore content is to remove as much gas from the melt as possible. Conversely, gas supersaturation of the melt is actually a precondition for the production of porous materials by the liquid metallurgy route. Shapovalov [1] applied a novel method to produce porous metals with ordered structure named gasars. The most important feature of the method is unidirectional solidification of a gas saturated melt that causes simultaneous formation of solid metal and gas pores resulting in an ordered gas-eutectic composition. This phase transformation is similar to the conventional eutectic reaction but one of the phases in the resulting eutectic structure is a gaseous phase, Fig. 1 [2]. The geometrical characteristics of the gas pores in gasar materials can be controlled in a wide range through a judicious selection of processing parameters [3], Fig. 2. This ordered structure provides attractive mechanical, thermal, tribological and other properties. Usually, the utilized gas is hydrogen but oxygen and nitrogen can also be selected. Other authors [4–6] used mixture of Ar and H_2 in different proportions as environment. Ar does not dissolve in liquid metal but the application of such gas mixture allows the formation of porosity to be controlled more flexibly. The porous materials considered possess combinations of unique properties such as exceptionally low weight, gas and liquid permeability, special acoustic characteristics, high damping capacity for absorption of mechanical energy.

Whereas ordered porosity materials have been extensively studied in the last decade in view of their unusual properties and potential applications, there has been a lack of fundamental understanding of their formation process. Predominantly mathematical models related to gasars describe the structure influence on some mechanical properties [7–9]. Shapovalov [3] gave simple mathematical descriptions of some particular details of the structure formation process. Sridhar and Russell [10], and Apprill [4] discussed pore nucleation on pits and cracks of non-wetted inclusions in the melt. A model of the gasar structure formation in closed form is given in [11]. Here a more explicit and detailed description of simultaneous growth of solid and gas phases will be discussed. It has an emphasis on conditions for pore size changes and pore growth and closing.

*Author to whom all correspondence should be addressed.

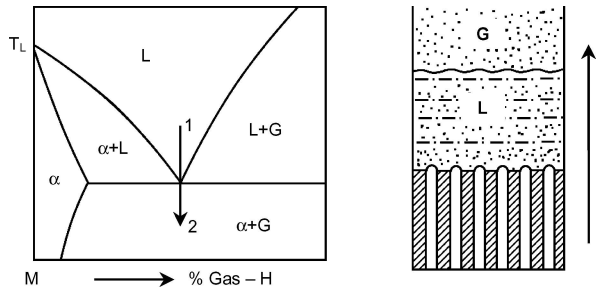

Figure 1 Typical phase equilibrium diagram for metal (M)—hydrogen (G) system (left) and eutectic growing upward in directional solidification (right), L—liquid state [2].

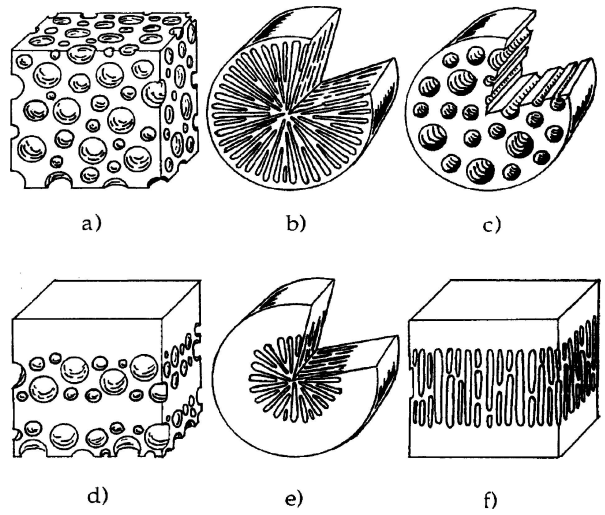

Figure 2 Diagrams of pore morphologies potentially available with the gasar process: spherical (a), radial (b), cylindrical (c), and laminates (d–f) [12].

2. Mathematical model

Both heat transfer and gas diffusion can be described by partial differential equations. To provide a unique solution for such equations, the physical area of the process evolution, and initial and boundary conditions have to be strongly defined.

2.1. Heat conduction

The temperature field $T = T(x, y, z, t)$ in both solid (gasar) and liquid (gas saturated melt) regions of the ingot is determined by the heat conduction equation:

$$c_{\text{eff}} \frac{\partial T}{\partial t} = \text{div}(\lambda \text{ grad } T) \tag{1}$$

where c_{eff} and $\lambda = \lambda(x, y, z, T)$ are specific heat and thermal conductivity, respectively. Detailed description of the heat transfer model and its application is given in [11].

2.2. Gas diffusion

One of the most important preconditions for the gas-eutectic reaction considered is a high level of gas supersaturation of liquid metal. Gas concentration near or above eutectic value C_{E} has to be provided (see Fig. 1). Gas diffusion in the melt appears because of the non-uniform gas distribution formed during the unidirectional solidification. The gas diffusion problem is considered only in the melt because diffusion in the solid formed does not affect significantly the structure. Stirring in the liquid is assumed to be negligible. The dynamics of gas concentration in liquid $C_{\text{L}} = C_{\text{L}}(x, y, z, t)$ is determined by the diffusion equation

$$\frac{\partial C_{\text{L}}}{\partial t} = \text{div}(D_{\text{L}} \text{ grad } C_{\text{L}}) \tag{2}$$

with initial condition

$$C_{\text{L}}(x, y, z, 0) = C_0 = K_{\text{L}} \sqrt{P_{\text{H2}}(0)} \tag{3}$$

Here, C_0 is initial gas distribution in the melt, P_{H2} is initial partial hydrogen pressure above the melt and $D_{\text{L}} = D_{\text{L}}(x, y, z)$ is diffusion coefficient of gas (H_2) in the liquid phase. Condition (3) expresses Sievert's law in case of constant temperature. Boundary conditions are as follows (see Fig. 3):

- on melt free surface, using Sievert's law,

$$C_{\text{L}}(x, y, H, t) = K_{\text{L}} \sqrt{P_{\text{H2}}(t)} \tag{4}$$

- on solid/liquid (S/L) interface (solidification front),

$$\frac{\partial C_{\text{L}}(x, y, 0, t)}{\partial z} = -A_2 \frac{V_{\text{cr}}(C_{\text{L}}(x, y, 0, t) - K_{\text{S}}) \sqrt{P_0(t)}}{D_{\text{L}}} \tag{5}$$

- on gas/liquid interface (boundary between pore and melt),

$$C_{\text{L}}(x, y, 0, t) = K_{\text{L}} \sqrt{P_{\text{H2}}(t)} + P_{\text{Ar}}(t) + \rho \text{gh} \tag{6}$$

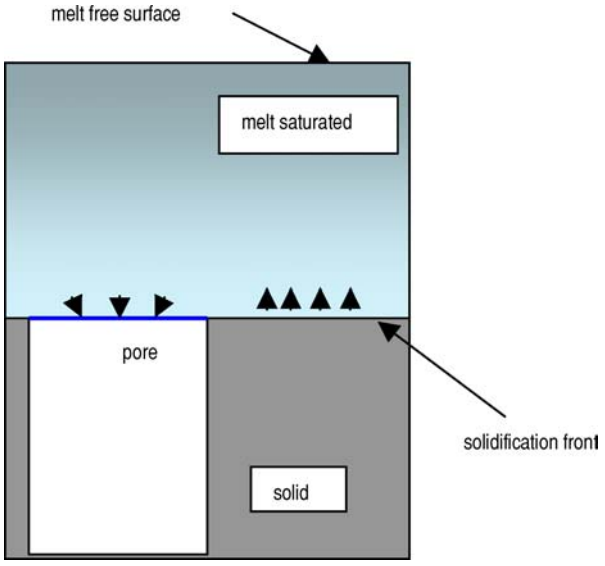

Figure 3 Schematic section of solid, liquid and gas phases in the gas-eutectic reaction.

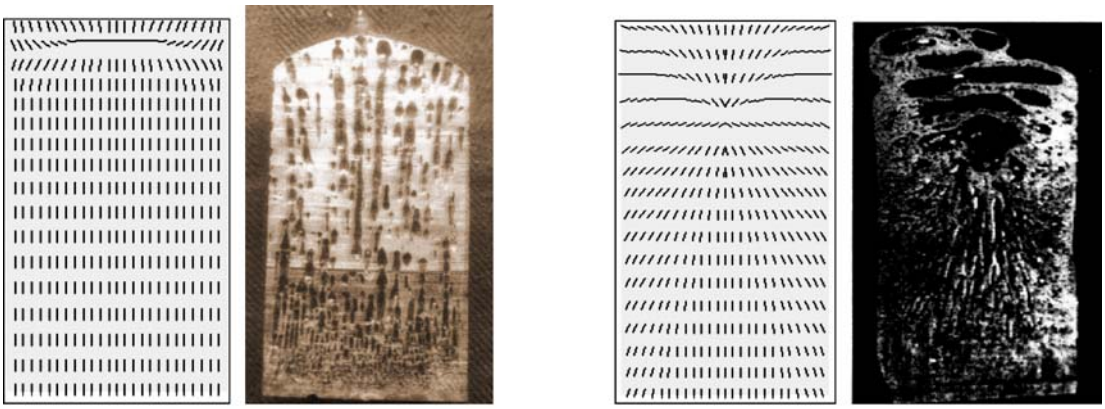

Figure 4 Pore directions obtained by numerical simulation (left) compared with real castings (right): (a) cooling of the casting runs predominantly through the bottom casting surface and (b) the heat flow through the casting surrounding surface is comparable with the heat flow through the bottom casting surface (on the example of copper gasars).

where K_L and K_S are Sievert's constants of hydrogen for liquid and solid respectively, $P_{H2}(t)$ and $P_{Ar}(t)$ are partial pressure of hydrogen and argon in gas mixture above the melt and V_{cr} is moving velocity of solid/liquid interface, ρ is the density and h is the height of liquid. Condition (5) expresses that the quantity of gas "injected" on S/L interface is proportional to the difference between the quantity of gas dissolved in liquid, $C_L(x, y, 0, t)$, and that dissolved in solid. Boundary condition (6) is defined also by Sievert's law but here it is taken into account that gas pressure in the pore is the sum of partial gas pressure of H_2 and Ar above the melt and hydrostatic pressure. A reasonable condition on vertical boundary of the liquid area is that the gas mass flow through it is zero,

$$\text{grad}C_L(x, y, z, t)|_{\text{boundary}} = 0 \qquad (7)$$

The Equation 2 and conditions (3)–(7) define completely gas field in the melt. The velocity V_{cr} in (5) is the joining element between thermal and diffusion problems.

3. Results and discussion

The mathematical model described above was applied for computer simulation of gas-eutectic transformation in gas saturated copper melt. At all numerical experiments pores are generated randomly on the S/L interface and Z axis is directed upward. Qualitative and quantitative information for the sensitivity of the gasar structure to the main processing parameters, both thermal and gas-diffusional, was obtained. Several types of numerical experiments were done.

At the first experiment pore direction was obtained. The fact that pore direction coincides with the thermal gradient on the solidification front [11] was used in calculations. If the cooling is essentially through the bottom, the pore directions are homogeneous all over the solid volume and coincide with longitudinal axis of the ingot, Fig. 4a. If the heat flow through the casting surrounding surface is comparable with the heat flow through the bottom surface of the casting, a non-homogeneous distribution of the pore directions appears, Fig. 4b. The model simulates these relationships adequately.

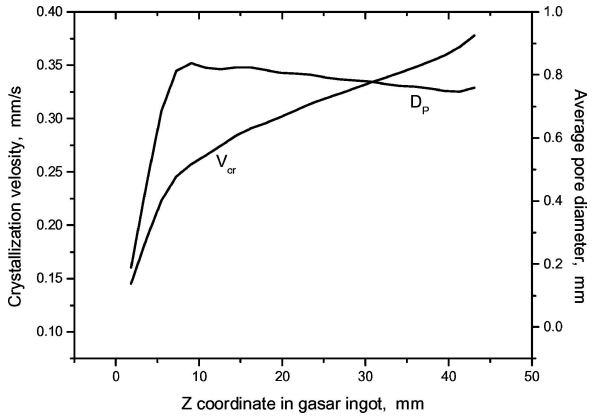

Figure 5 Calculated solidification velocity and average pore-diameter in a typical processing regime.

Average pore diameter and solidification velocity in a typical gasar process are shown in Fig. 5. It is normal to expect V_{cr} to increase during solidification. A rapid increasing is prohibited because the porous solid phase formed enlarges and heat transfer coefficient of the medium is relatively low. The average pore diameter increases sharply at the beginning of structure formation and then stays approximately constant.

Influence of Ar and H_2 partial gas pressure, P_{Ar} and P_{H_2} respectively, on the pore shape and size was investigated in the third type of experiments. Fig. 6a depicts the minimal, $D_{P\,min}$, maximal, $D_{P\,max}$, and average, $D_{P\,av}$, pore diameters formed under initial $P_{Ar} = 0.20$ MPa and $P_{H_2} = 0.30$ MPa, and rapid increasing of P_{Ar} after 80 sec from 0.20 to 0.25 MPa, Fig. 6b. The rapid increasing of gas pressure causes big decreasing of pore diameters in a narrow depth, and after this the pore diameters stabilize again on lower size. The same correlation is valid in case of P_{H_2} increasing from 0.30 MPa to 0.35 MPa, Figs 6c and d. Here the average pore diameter (after reduction) is greater than at the previous case because hydrogen concentration in liquid is greater according to Sievert's law. The $D_{P\,av}$(Ar) curve in Fig. 6c

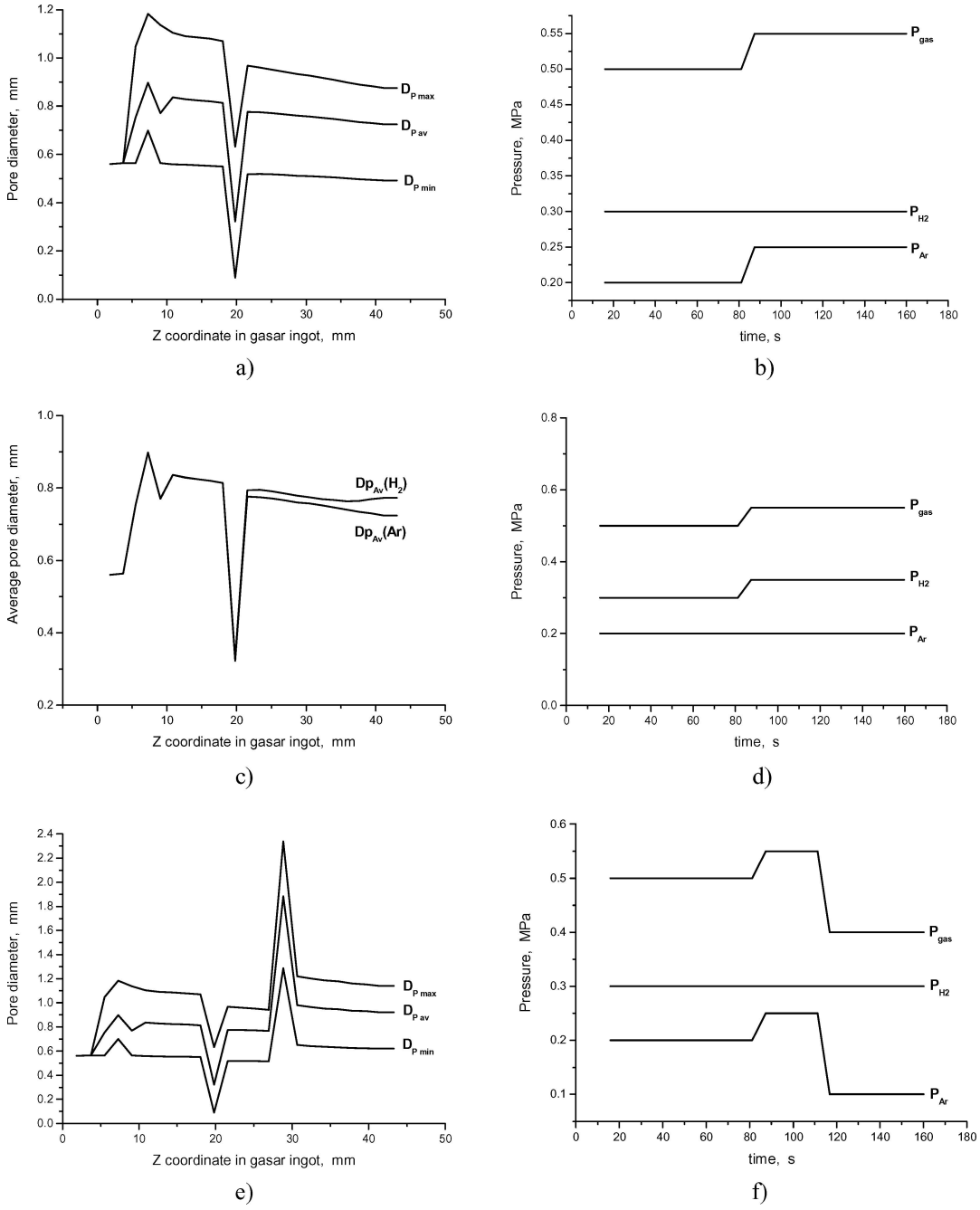

Figure 6 Influence of partial gas pressure on pore formation.

is reproduced from the $D_{\mathrm{P\,av}}$ line in Fig. 6a. The minimal, maximal and average pore diameters in gasar ingot formed under increasing and decreasing of P_{Ar}, Fig. 6f, is shown in Fig. 6e.

4. Summary and conclusions

The mathematical model presented here provides the possibility of accurate numerical simulation of the gasar technology. Using the model, quantitative information for the sensitivity of the gasar structure to the main processing parameters can be obtained. The software product enables calculation of the temperature field during structure formation, porosity content, pore direction, gas bubble nucleation and four local criteria. The basic conclusions can be summarized as follows:

[1.] The gasar structure depends on external gas pressure, solidification velocity and gas concentration in the liquid in a complicated and non-linear way. Rapid changes in gas pressure cause rapid changes of pore diameter in narrow depth;

[2.] Manipulation of partial argon and/or hydrogen pressure allows flexible control of pore size and shape over a wide interval.

Acknowledgment

This work was supported by the Bulgarian National Science Fund (Contract No. TH1313) and Polish Ministry of Scientific Research and Information Technology (Grant No. T08 B 014 19).

References

1. V. I. SHAPOVALOV, Method for Manufacturing Porous Articles, U.S. Patent No.5181549 (Jan. 26, 1993).

2. V. I. SHAPOVALOV, *Porous Metals, MRS Bulletin* April (1994) 24.
3. V. I. SHAPOVALOV, in Porous and Cellular Materials for Structural Applications, Materials Research Society Symposium (Materials Research Society: Pittsburgh PA, 1998) vol. 521, p. 281.
4. J. M. APPRILL, D.R. POIRIER, M.C. MAGUIRE and T. C. GUTSCH, in Porous and Cellular Materials for Structural Applications, Materials Research Society Symposium (Materials Research Society, Pittsburgh, PA, 1998) vol. 521, p. 291.
5. C. J. PARADIES, A. TOBIN and J. WOLLA, in Porous and Cellular Materials for Structural Applications, Materials Research Society Symposium (Materials Research Society, Pittsburgh, PA, 1998) vol. 521, p. 297.
6. H. NAKAJIMA, S.K. HYUN, K. OHASHI, K. OTA and K. MURAKAMI, *Colloid Surf. A-Physicochem. Eng. Asp.* **179** (2001) 209.
7. R. J. BONENBERGER, A. J. KEE, R. K. EVERETT and P. MATIC, in Porous and Cellular Materials for Structural Applications, Materials Research Society Symposium (Materials Research Society, Pittsburgh, PA, 1998) vol. 521, p. 303.
8. V. PROVENZANO, J. WOLLA, P. NATIC, A. GELTMACHER and A. KEE, in Advances in Porous Materials, Materials Research Society Symposium (Materials Research Society, Pittsburgh, PA, 1995) vol. 371, p. 383.
9. A. E. SIMONE and L. J. GIBSON, *Acta Mater.* **44** (1996) 1437.
10. S. SRIDHAR and K. C. RUSSELL, *J. Mater. Synthesis and Proc.* **3** (1995) 215.
11. L. DRENCHEV, J. SOBCZAK, R. ASTHANA and S. MALINOV, *Computer-Aided Materials Design* **10** (2003) 35.
12. D. M. VALUKAS, Internal Report, Ann Arbor (MI): USP Holdings (1992).

Received 31 March
and accepted 20 October 2004